CODEN IEJMAT *Internet Electronic Journal of Molecular Design* **2007**, *6*, 70–80 ISSN 1538–6414
BioChem Press http://www.biochempress.com

Inter*net* Electronic Journal of Molecular Design

March 2007, Volume 6, Number 3, Pages 70–80

Editor: Ovidiu Ivanciuc

Special issue dedicated to Professor Lemont B. Kier on the occasion of the 75th birthday

A DFT Study on the Low–Lying Excited States and Adiabatic Photodissociation Channels of Nitric Acid

Costantino Zazza [1,2] and Luigi Bencivenni [3]

[1] Consorzio interuniversitario per le Applicazioni di Supercalcolo Per Università e Ricerca (CASPUR), via dei Tizii 6b, 00185 Roma, Italy
[2] Dipartimento di Chimica, Ingegneria Chimica e Materiali, Università de l'Aquila, via Vetoio (Coppito 1), 67010 l'Aquila, Italy
[3] Dipartimento di Chimica, Università di Roma "La Sapienza", P.le Aldo Moro 5, 00185 Roma, Italy

Received: September 19, 2006; Revised: November 13, 2006; Accepted: December 21, 2006; Published: March 31, 2007

Citation of the article:
C. Zazza and L. Bencivenni, A DFT Study on the Low–Lying Excited States and Adiabatic Photodissociation Channels of Nitric Acid, *Internet Electron. J. Mol. Des.* **2007**, *6*, 70–80, http://www.biochempress.com.

Inter*net* **Electronic** Journal of Molecular Design

BioChem Press
http://www.biochempress.com

A DFT Study on the Low–Lying Excited States and Adiabatic Photodissociation Channels of Nitric Acid

Costantino Zazza [1,2,*] and Luigi Bencivenni [3]

[1] Consorzio interuniversitario per le Applicazioni di Supercalcolo Per Università e Ricerca (CASPUR), via dei Tizii 6b, 00185 Roma, Italy
[2] Dipartimento di Chimica, Ingegneria Chimica e Materiali, Università de l'Aquila, via Vetoio (Coppito 1), 67010 l'Aquila, Italy
[3] Dipartimento di Chimica, Università di Roma "La Sapienza", P.le Aldo Moro 5, 00185 Roma, Italy

Received: September 19, 2006; Revised: November 13, 2006; Accepted: December 21, 2006; Published: March 31, 2007

Internet Electron. J. Mol. Des. **2007**, *6* (3), 70–80

Abstract

Motivation. In this paper, the lowest valence electronic excited states of nitric acid (HNO_3) have been computed by means of density functional theory within its time dependent formalism and compared with experimental data and previous first principles calculations. Further, since nitric acid plays an important role in atmosphere providing an important source of stratospheric OH radical, due to its rapid photo–dissociation, the lowest adiabatic photo–dissociation channels have been also studied.

Method. Time dependent density functional theory (TD–DFT) with different functionals, in conjunction with different basis sets, has been applied to calculate the vertical transition energies from the ground state to the low–lying singlet and triplet electronic excitated states of nitric acid in vacuum. Moreover, the adiabatic photo–dissociation channels of HNO_3 molecule into $OH\cdot + NO_2\cdot$ were investigated sampling the potential energy surfaces (PES) of the lowest singlet excited states at TD–DFT(B3LYP)/aug–cc–pVQZ level of theory.

Results. This work, one more time, confirms that the TD–DFT based calculations, together with generalized gradient–corrected approximation (GGA), provide accurate and physically consistent description of the lowest valence electronic excitation transitions. Moreover, in line with our previous results on hexafluoropropene, the comparison with more expensive calculations, such as MRDCI, CIS(D), CASSCF, MCQDPT and CCSD, clearly shows the excellent performance of the TD–DFT formalism with highly correlated systems with a limited extent of multiple excitation character.

Conclusions. Our TD–DFT results are in satisfactory agreement with UV experimental absorption bands and in analogy with previous results obtained by means of high level calculations. Interestingly, in this work we show that at 248 nm, the potential energy barrier toward dissociation of the acid nitric in OH + NO_2 radical fragments strongly depends on the out–of–plane bending vibration of the molecule in the 1 ^{1}A" excited state having a noticeable contribution to the lowering of the barrier.

Keywords. Nitric acid; vertical excited states; adiabatic photo–dissociation channels.

Dedicated to Professor Lemont B. Kier on the occasion of the 75th birthday.

* Correspondence author; phone: +39–06–44486720; fax: +39–06–4957083; E–mail: costantino.zazza@caspur.

1 INTRODUCTION

Recently, photodissociation of hexafluoropropene [1] was studied using time dependent density functional theory (TD–DFT) with some success. In that work, the computational advantages of the DFT theory in dealing with these processes are exposed.

Photochemistry of nitric acid (HNO_3) in the UV region was examined theoretically [2–4], as well as experimentally [5–7], by several authors because OH radical is the most important photo–dissociation product in atmosphere. Gas phase reactions of OH radical with alkenes and aromatic molecules are quite important in stratospheric chemistry [8]. The photodissociation channels are also particularly interesting in computational chemistry because they offer the opportunity to test the accuracy of high level quantum chemical procedures for small and relatively large size molecules. Density functional theory (DFT) [9] with its time dependent formalism [10,11] provides a valuable performance in the determination of vertical excitation energies and adiabatic photo–dissociation channels [12–15].

Prompted from the same aim, we have thought to extend this computational approach to validate the proposed valence assignments for the lowest singlet and triplet excited states of acid nitric based on CIS, CIS(D), CCSD and MRD–CI calculations [2,3] through density functional theory (DFT) as an alternative tool. The success of density functional theory is quite important in this respect in view of its use for studying larger molecules in gas phase. The further aim of this work is the determination of OH–NO_2 binding energy as well as the adiabatic photo–dissociation channels which provides OH· and NO_2· radicals.

The paper is organized as follows: in the next session we show the computational approaches used to investigate the low–lying singlet and triplet electronic excited states and the lowest adiabatic photodissociation channels (section 2) of the nitric acid. Afterwards, (section 3), vertical excitation energies and lowest potential energy surfaces are discussed and compared with experimental data and previous first principles calculations. Finally, in the section 4, the general conclusions of this work are exposed.

2 MATERIALS AND METHODS

Geometry optimizations and TD calculations on HNO_3 molecule were carried out using the following gradient–corrected approximation (GGA) based functionals: B3LYP [16–18], BLYP [17,18], PBE1PBE [19–21] and PW91 [22]. The Dunning's correlation consistent basis sets, augmented with diffuse functions for all atoms, aug–cc–pVDZ, aug–cc–pVTZ and aug–cc–pVQZ, were used for all the calculations [24,25]. Time dependent density functional (TD–DFT) calculations were performed using the same functional–basis set combination at the corresponding optimized structure to obtain vertical excitation energies from the ground state energy to different

low–lying singlet and triplet excited states of HNO_3 molecule.

In order to verify the performance of the time–dependent formalism, complete active space self–consistent reaction field (CASSCF) and multi–configuration quasi–degenerate perturbation theory (MCQDPT) calculations were carried out using an active space consisting of eight electrons in ten molecular orbitals [26]. The basis set chosen for these further computation was the 6–311++G(2d,2p) for all atoms [27].

At last, the adiabatic photo–dissociation channels of HNO_3 molecule into $OH\cdot + NO_2\cdot$ were investigated. For this purpose, one had to sample the potential energy surfaces (PES) of the lowest singlet excited states along the generalized coordinate leading to the dissociation process. In this respect, the three lowest singlet excited states were sampled at the TD–DFT(B3LYP)/aug–cc–pVQZ level of theory. The $HO–NO_2$ bond length was varied starting from its optimized value 1.409 Å at the same level of the theory (B3LYP/aug–cc–pVQZ) up to 2.45 Å. At each point of the ground state geometry, the orthogonal nuclear degrees of freedom were relaxed and the vertical transition energy values were recalculated. Note that the same computational methodology was successfully applied in an our previous work [1].

The DFT studies were accomplished with the GAUSSIAN package [28] and the GAMESS–US [29] was used for the CASSCF and MCQDPT computations. Calculations were performed on a 4–way HP Proliant–DL585 server with dual–core AMD Opteron Processor 850 running at 2.4 GHz.

3 RESULTS AND DISCUSSION

3.1 Low–Lying Singlet and Triplet Electronic Excited States

The singlet vertical excitation energies of nitric acid were studied using the BLYP, B3LYP, PBE1PBE and PW91 density functionals with the aug–cc–pVDZ, aug–cc–pVTZ, and aug–cc–pVQZ basis sets.

The $1^1A'$ ground state equilibrium geometry of the molecule does not depend on the level of the calculation appreciably. As a matter of fact, all the combinations of the density functionals and atomic basis sets provide a C_s absolute minimum with 1A' character and the difference in terms of internal coordinates are less than the five per cent. In correspondence of the optimized geometry, at each level of the DFT theory, the vertical singlet and triplet transition energies were evaluated using the DFT with the time–dependent formalism (TD–TDF). It is valuable before plunging into the discussion of the results to take into account the molecular orbitals involved in the lowest valence electronic transitions that are going to be examined. In Figure 1, the plots of these electronic transitions are represented in the suitable molecular orbital view. From this representation, one may realize that these electronic transitions have a strong $^1n \rightarrow \pi^*$ and $^1\pi \rightarrow \pi^*$ character, being mainly

localized on the NO_2 moiety of the molecule, thus confirming the previous assignments [2–4]. Within the DFT approach, the first 1A" excited state is basically due to the HOMO → LUMO electronic excitation from the 16th to the 17th molecular orbital whilst the next excited state 2^1A" originates from the HOMO–2 → LUMO transition occurring from the 14th to the 17th molecular orbital.

The next excited states retain the character of the wave–function of the electronic ground state and more precisely the third 2^1A' excited state mainly involves an electronic transition from the HOMO–3 → LUMO molecular orbital (from the 13rd to the 17th molecular orbital) and the fourth 3^1A' excited electronic state involves an electronic HOMO–1 → LUMO transition, from the 15th to the 17th molecular orbital. Roughly speaking, the 13rd, 14th, 15th and 16th occupied molecular orbitals reveal π bonding localized on the NO_2 group, non–bonding on the O atom, π bonding, non–bonding on the O atom and π* anti–bonding, respectively.

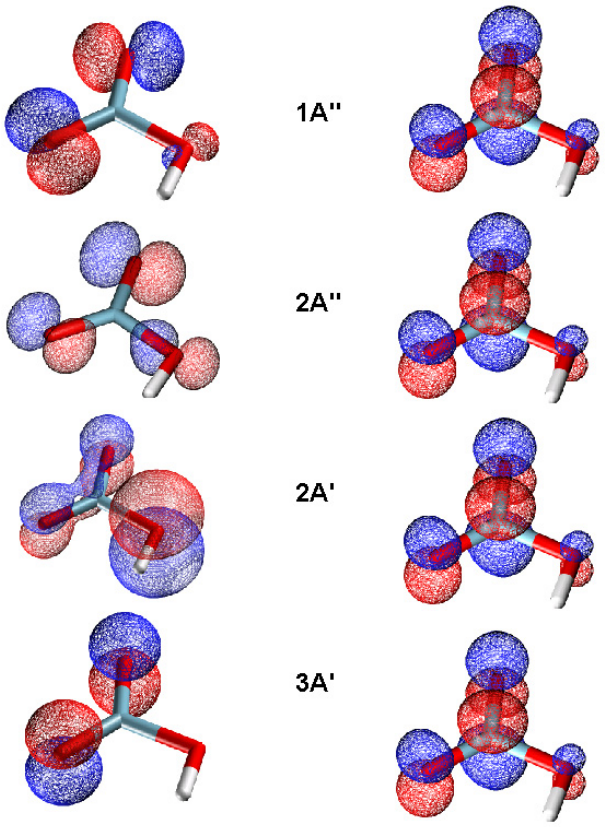

Figure 1. Molecular orbitals mainly involved in the first four valence electronic transitions (1 ^{1}A", 2 ^{1}A", 2 ^{1}A' and 3^{1}A') of nitric acid.

The character of the molecular orbitals involved in the excitation process determined through the calculations are in agreement with previous quantum chemical calculations at CIS/6–31G*, CCSD/6–31G* and MRD–CI/DZPR levels of theory [2,3]. The TD–DFT results of the calculated singlet transitions are collected in Table 1.

Table 1. Singlet Excited States of Nitric Acid: Vertical Excitation Energies (eV) and Oscillator Strengths (Dimensionless); Average Energy Values Are Reported Along with Standard Deviation

Method	$^1n \rightarrow \pi^*$	$^1n \rightarrow \pi^*$	$^1\pi \rightarrow \pi^*$	$^1\pi \rightarrow \pi^*$
B3LYP/aug–cc–pVDZ	4.75	5.72	7.01(0.038)	7.20(0.090)
B3LYP/aug–cc–pVTZ	4.86	5.80	7.07(0.035)	7.27(0.087)
B3LYP/aug–cc–pVQZ	4.85	5.82	7.11(0.038)	7.30(0.087)
average	4.82 ± 0.06	5.78 ± 0.05	7.06 ± 0.05	7.26 ± 0.05
PBE1PBE/aug–cc–pVDZ	4.91	5.96	7.41(0.087)	7.57(0.094)
PBE1PBE/aug–cc–pVTZ	5.01	6.03	7.47(0.083)	7.63(0.094)
PBE1PBE/aug–cc–pVQZ	5.02	6.04	7.49(0.089)	7.65(0.090)
average	4.98 ± 0.06	6.01 ± 0.04	7.46 ± 0.04	7.62 ± 0.04
BLYP/aug–cc–pVDZ	4.51	5.32	5.86(0.020)	7.49(0.138)
BLYP/aug–cc–pVTZ	4.62	5.39	5.87(0.019)	7.58(0.144)
BLYP/aug–cc–pVQZ	4.63	5.41	5.92(0.020)	7.58(0.136)
average	4.59 ± 0.07	5.37 ± 0.05	5.88 ± 0.03	7.55 ± 0.05
PW91/aug–cc–pVDZ	4.60	5.49	6.18(0.025)	7.66(0.101)
PW91/aug–cc–pVTZ	4.70	5.56	6.20(0.026)	7.75(0.123)
PW91/aug–cc–pVQZ	4.70	5.57	6.24(0.026)	7.77(0.113)
average	4.67 ± 0.06	5.54 ± 0.03	6.21 ± 0.03	7.73 ± 0.06
average DFT (GGA)	**4.76 ± 0.16**	**5.67 ± 0.25**	**6.65 ± 0.66**	**7.54 ± 0.19**
CASSCF(8,10)/6–311++G(2d,2p)	5.14	6.20		
MCQDPT/6–311++G(2d,2p)	4.90	6.15		
previous calculations [2,3]				
CIS/6–311(2+,2+)G**	5.63	6.51	7.84(0.342)	9.87(0.026)
CIS(D)/6–311(2+,2+)G**	4.71	5.73	6.92	7.09
CCSD/6–311(2+,2+)G**	4.78	5.80	7.01	7.66
MRDCI/DZP(6d)R(sp)	4.59	5.59	6.88(0.3)	
experimental [30,31]	4.59	5.90	6.71	

From these theoretical data, one may see that the two lowest $^1n \rightarrow \pi^*$ and $^1\pi \rightarrow \pi^*$ electronic transitions both depend on the density functional and the basis set, although the calculated values reproduce satisfactory the experimental sequence, namely $^1n \rightarrow \pi^*$ 4.6 and 5.9 eV and $^1\pi \rightarrow \pi^*$ 6.7 eV [30,31]. The best DFT result was accomplished for the lowest $^1n \rightarrow \pi^*$ electronic transition from both the PW91/aug–cc–pVDZ level, that is 4.60 eV, against its experimental determination at 4.59 eV [30,31]. The best estimate of the next $^1n \rightarrow \pi^*$ electronic transition, reported at 5.90 eV [30,31], is that provided from the PBE1PBE/aug–cc–pVDZ level (5.96 eV) and the best agreement for the lowest valence $^1\pi \rightarrow \pi^*$ electronic transition measured at 6.71 eV is obtained from the B3LYP/aug–cc–pVDZ estimate, 7.01 eV. The least difference between the experimental and the calculated value is +0.01 eV for the lowest energy $^1n \rightarrow \pi^*$ transition calculated at the PW91/aug–cc–pVDZ level (4.60 eV) and –0.8 eV for the $^1\pi \rightarrow \pi^*$ transition calculated at the BLYP/aug–cc–pVDZ level (5.86 eV). As one may deduce from the data reported in Table 1, the basis set effect, within each DF used, is not particularly large and in general the largest basis set, the aug–cc–pVQZ, always provides the highest energy value for all the calculated electronic transitions. In other words, the aug–cc–pVQZ basis set overestimates the vertical excitation energies of the two lowest $^1n \rightarrow \pi^*$ transitions by 0.1 eV with respect to the aug–cc–pVDZ less extended basis set.

One might also propose an average vertical excitation energy value determined for each density functional (see Table 1), more suitably. In doing this, it emerges, except for the highest energy $^1\pi \rightarrow$

π* transition, that the BLYP level provides the lowest excitation energy, whereas the PBE1PBE level provides the highest excitation energy for the $^1n \rightarrow \pi^*$ and $^1\pi \rightarrow \pi^*$. For the highest energy $^1\pi \rightarrow \pi^*$ transition, the lowest and the highest estimate of the excitation energy occurs when the B3LYP and PW91 density functionals are employed. In summary, the DFT methods yield satisfactory estimates of the excitation energies (4.76 ± 0.16 and 5.67 ± 0.25 eV for the $^1n \rightarrow \pi^*$ transitions and 6.65 ± 0.66 and 7.54 ± 0.19 eV for the $^1\pi \rightarrow \pi^*$ transitions, respectively).

Earlier CIS, CIS(D), CCSD and MRD–CI calculations [2,3], employing the 6–31G* and 6–311(2+,2+)G** basis sets, provide for the $^1n \rightarrow \pi^*$ and the $^1\pi \rightarrow \pi^*$ electronic transitions values of the vertical excitation energies which largely depend on the computational level. Neglecting the 6–31G* data, the CIS method places the first two $^1n \rightarrow \pi^*$ transitions at 5.63 and 6.51 eV [3] overestimating them with regard to the experimental values 4.6 eV and 5.9 eV [30,31] . A noticeable improvement occurs when the CIS(D) (4.71 eV and 5.73 eV) and CCSD (4.78 eV and 5.80 eV) levels are adopted. The MRD–CI estimate with the DZPR basis set [2] further improves the agreement between theory and measure for the lower energy $^1n \rightarrow \pi^*$ transition (4.59 eV) with respect to the CIS(D) and CCSD calculations performed with the 6–311(2+,2+)G** basis set, although underestimates by 0.3 eV the higher energy $^1n \rightarrow \pi^*$ transition computed at 5.6 eV.

Table 2. Triplet Excited States of Nitric Acid: Vertical Excitation Energies (eV) and Oscillator Strengths (Dimensionless); Average Energy Values Are Reported Along with Standard Deviation

Method	$^3n \rightarrow \pi^*$	$^3n \rightarrow \pi^*$	$^3\pi \rightarrow \pi^*$	$^3\pi \rightarrow \pi^*$
B3LYP/aug–cc–pVDZ	4.16	5.23	3.93	5.88
B3LYP/aug–cc–pVTZ	4.27	5.31	4.03	5.98
B3LYP/aug–cc–pVQZ	4.28	5.33	4.04	6.01
average	4.24 ± 0.07	5.29 ± 0.05	4.00 ± 0.06	5.96 ± 0.07
PBE1PBE/aug–cc–pVDZ	4.29	5.42	3.98	6.18
PBE1PBE/aug–cc–pVTZ	4.38	5.49	4.06	6.27
PBE1PBE/aug–cc–pVQZ	4.39	5.51	4.07	6.29
average	4.35 ± 0.06	5.47 ± 0.05	4.04 ± 0.05	6.25 ± 0.06
BLYP/aug–cc–pVDZ	3.96	4.87	4.17	4.96
BLYP/aug–cc–pVTZ	4.07	4.95	4.27	5.01
BLYP/aug–cc–pVQZ	4.09	4.97	4.26	5.04
average	4.04 ± 0.07	4.93 ± 0.05	4.23 ± 0.06	5.00 ± 0.04
PW91/aug–cc–pVDZ	4.03	5.02	4.31	5.18
PW91/aug–cc–pVTZ	4.13	5.09	4.39	5.23
PW91/aug–cc–pVQZ	4.15	5.11	4.40	5.26
average	4.10 ± 0.06	5.07 ± 0.05	4.37 ± 0.05	5.22 ± 0.04
average DFT (GGA)	**4.18 ± 0.14**	**5.19 ± 0.22**	**4.16 ± 0.16**	**5.61 ± 0.53**
previous calculations [3]				
CIS/6–311(2+,2+)G**	5.00	5.96	3.49	7.50
CIS(D)/6–311(2+,2+)G**	4.46	5.58	4.63	7.74
QCISD/6–31G*	4.46		4.33	
QCISD(T)/6–31G*		4.96	5.04	
experimental [30,31]	4.59	5.90	6.71	

In order to further verify the performance of the TD–DFT formalism and the available functionals in the investigation of the electronic transitions, a more correlated and expensive

MCQDPT/CASSCF(8,10)/6–311++G(2d,2p) calculation [26] was carried out including the two lowest 1 ^{1}A" and 2 ^{1}A" singlet excited states. From the data collected in Table 1, it is of interest to note that, at fixed geometry, (CASSCF(8,10)/6–311++G(2d,2p) optimized geometry was used), the excited states benefit preferentially, with respect to the ground state, after the explicit inclusion of the dynamical correlation, by means of perturbation theory (MCQDPT). However, from the comparison with TD–DFT results it clearly emerges that the MCQDPT and CASSCF approaches provide an upper limit for these estimates, above 5.0 eV and 6.0 eV for the ^{1}n → π* transitions.

Regarding the lowest triplet excited states, Table 2 summarizes the vertical excitation energies of the ^{3}n → π* and the ^{3}π → π* transitions determined using different density functionals.

The two lowest ^{3}A" excited states would relate to the two lowest ^{1}A" excited states being n → π* transitions and the two lowest ^{3}A' excited states would relate to the two distinct ^{1}A' singlet excited states being π → π* transitions basically of the NO_2 group. Unfortunately, one cannot assess the validity of the DFT calculations against the previous ones [3] performed at the CIS and CIS(D) levels with the 6–311(2+,2+)G** basis set because no experimental data are known for these electronic transitions. If one bases the discussion on the average vertical excitation energy values, that is 4.18 ± 0.14 and 5.19 ± 0.22 eV for the ^{3}n → π* and 4.16 ± 0.16 and 5.61 ± 0.53 eV for the ^{3}π → π* transitions, it appears that the CIS and CIS(D) methods provide higher excitation energy values than the DFT ones, notwithstanding the fact that CIS(D) level data are closer to the DFT estimates, with the exception of the highest energy ^{3}π → π* transition at 7.74 eV which seems not to dependent on the CI approximation.

The main difference with respect to the analysis already reported in literature [3] is that, according to the DFT description of the molecular orbitals of the electronic ground state, the lowest ^{1}π → π* transitions have reversed energies. Furthermore, the oscillator strengths computed for both these transitions strongly depend on the density functional and basis set (see Table 1) and therefore, only qualitative information can be reached from the oscillator strength values. The band intensity of the higher energy ^{1}π → π* transition would be larger than that expected for the lower energy one, this conclusion based on the density functional however does not agree with the CIS/6–311(2+,2+)G** calculations providing an opposite intensity pattern. It is not possible, on this ground, to invalidate the alternative assignment of these transitions proposed earlier through CIS/6–311(2+,2+)G** calculations [3]. At the same time, the experimental result does not allow to reach any conclusion since the measured electronic transitions produce an intense but “broad” absorption band centered at 185 nm (6.70 eV).

At last, turning to the binding energy, in order to further confirm the hypothesis of the dissociation process through the cleavage of HNO_3 to form $OH^{\cdot}$ + $NO_2^{\cdot}$, we have calculated the

energetic of this process considering the products in their own ground states. These calculations were performed with the gradient–corrected approximation (GGA) with the B3LYP, PBE1PBE, BLYP and PW91 density functionals using the aug–cc–pVQZ basis set, being the performance of these functionals well known for this task [32]. The average DFT(GGA) harmonically zero point vibrational corrected binding energy D_0^h (HO–NO_2) value is 197.8 kJ mol^{-1}, in agreement with the experimental one 198.7 kJ mol^{-1} [33]. These results are reported in Table 3.

Table 3. HO–NO_2 counterpoise–corrected (cpc) and harmonically zero–point corrected binding energies D_e^{cpc} and D_0^h (kJ mol^{-1}). Basis set superposition error (BSSE) is reported in kJ mol^{-1} and average binding energy (D_0^h) value is reported along with standard deviation. Triplet excited states of nitric acid: vertical excitation energies (eV) and oscillator strengths (dimensionless). Average energy values are reported along with standard deviation.

Method	D_e^{cpc}	D_0^h	BSSE
B3LYP/aug–cc–pVQZ	205.4	182	0.7
PBE1PBE/aug–cc–pVQZ	225.1	200.4	0.7
BLYP/aug–cc–pVQZ	210.9	189.1	0.75
PW91/aug–cc–pVQZ	243.1	219.7	0.7
average DFT (GGA)		197.8 ± 16.4	
experimental [33]		198.7 ± 2.1	

3.2 Adiabatic Photo–dissociation Channels

According to the UV absorption spectrum of HNO_3, showing two broad peaks, the most intense one at 185 nm (6.70 eV) is due to both the $^1\pi \rightarrow \pi^*$ transitions and the other one at 270 nm (4.59 eV) is originating from the non–bonding oxygen atoms to the π^* orbital of the NO_2 moiety. The photodissociation channels at 193nm (6.42 eV), 248 nm (5.00 eV) and 280 nm (4.42 eV) leading to OH· and NO_2· fragments have been studied deeply both experimentally [2–4] and theoretically [5–7]. As already discussed elsewhere [4], the fragmentation of the molecule at the shorter wavelength may produce either NO_2· in the 1 $^2B_2$ or 2 $^2B_2$ excited electronic state. On this respect, photofragment translational energy measurements by Myers and co–workers showed a bimodal translational energy distributions for the OH· + NO_2· dissociation channel. One channel (the faster one) produces stable fragments with an average translational energy peaks at 146 kJ mol^{-1} and it has been assigned to OH· + NO_2· (1 $^2B_2$) on the basis of the adiabatic correlation diagram from the singlet excited state of nitric acid (1 $^1A'$) to OH + NO_2 asymptotic radical products. The slower channel, which provides a maximum at 63 kJ mol^{-1} (hence with the fragments at more internal energy) correlates nonadiabatically to NO_2 (2 $^2B_2$) excited state which undergoes secondary dissociation to NO· + O·. As a matter of fact, has been supposed that if the molecule does not follow the adiabatic pathway along the 2 $^1A'$ potential energy surface, the system hops on the 3 $^1A'$ hypersurface which leads to OH· + NO_2· (2 $^2B_2$) products [4].

On the basis of previous investigations [2–4], let us now consider the adiabatic photodissociation channel $HONO_2$ (1 $^1A'$) + hν → OH· ($^2\Pi$) + NO_2· (1 $^2A_1$ or 1 $^2B_2$). For this purpose, the potential

energy curves (PESs) of the first excited states (1 ^{1}A", 2 ^{1}A", 2 ^{1}A') were determined at the TD–DFT(B3LYP/aug–cc–pVQZ) level. During the 1 ^{1}A' ground state surface scanning, the HO–NO_2 bond length was varied from its equilibrium value 1.409 Å up to 2.450 Å and the orthogonal nuclear degrees of freedom were relaxed step by step, following the same computational procedure adopted for hexafluoropropene [1]. It is interesting to note that the lowest 1 ^{1}A" excited state provides a barrier (0.6 eV at 1.47 Å) toward the dissociation process whilst the 2 ^{1}A" and 2 ^{1}A' excited states cross one with the other at 1.75 Å, both showing a potential energy profile lacking of a meaningful barrier (Figure 2 and Figure 3). As matter of fact, at least within the explored range, the 2 ^{1}A" excited state has a quite flat energy profile but, on the contrary, the lowest 1 ^{1}A' shows a slight repulsive behavior along this internal degrees of freedom (see Figure 3). Previous quantum chemistry calculations [2] carried out for the same excited states showed that the minimum potential energy curves of the three lowest singlet excited states along the dissociation path have small barriers, namely 0.31 eV for the 1 ^{1}A", 0.14 eV for 2 ^{1}A" and 0.04 eV for the 1 ^{1}A'.

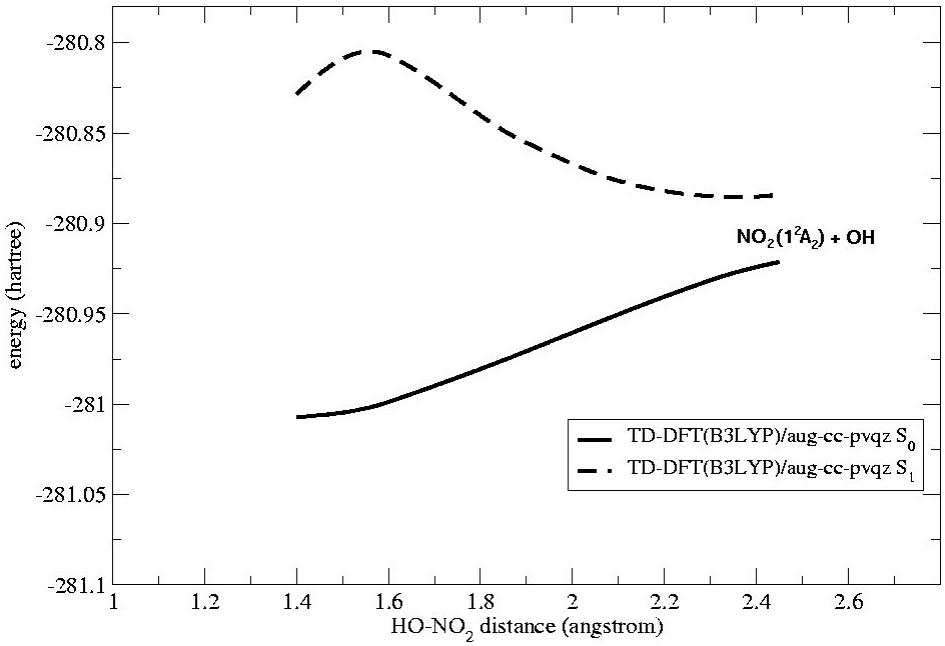

Figure 2. Potential energy curves of the ground (1 ^{1}A') and first (1 ^{1}A") valence excited state of acid nitric along the HO–NO_2 bond.

The equilibrium geometries of these three lowest excited states were found to be pyramidal with the NO_2 group bending down out of the ground state molecular plane and the hydrogen atom is rotated by 90° about the proper NO axis [2]. Our DFT computations confirm that the nuclear relaxation after the excitation process plays a crucial role along the lowest energy photodissociation channel. In fact, constraining the molecule to remain planar throughout the calculations, the bond dissociation barrier occurring on the 1 ^{1}A" excited surface is twice with respect to the value obtained for the non–planar geometry.

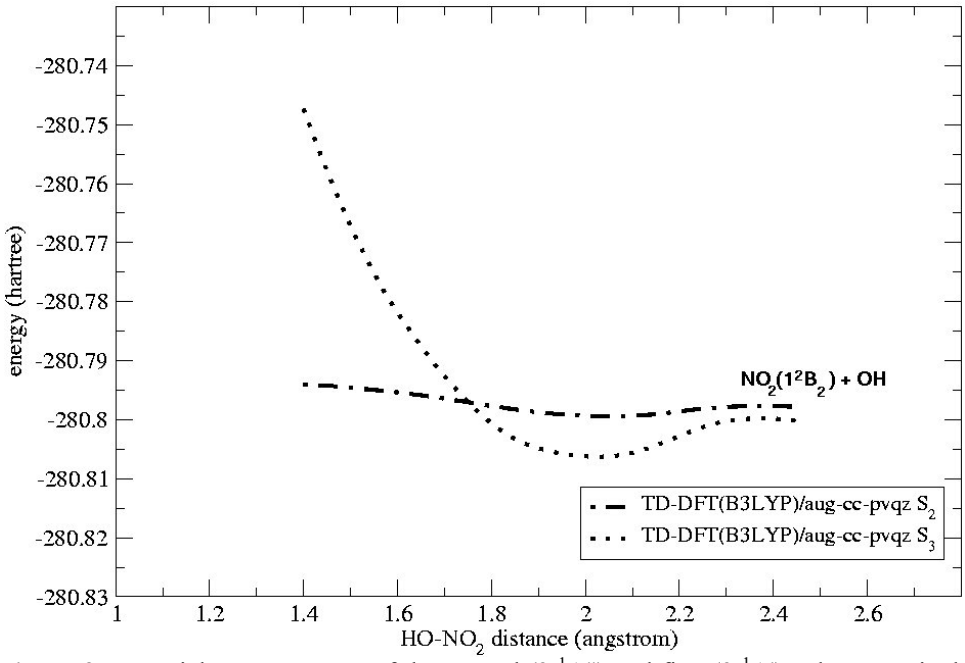

Figure 3. Potential energy curves of the ground (2 ^{1}A") and first (2 ^{1}A') valence excited state of acid nitric along the HO–NO_2 bond.

Interestingly enough, our results confirm that if the dissociation process at 280 nm takes place on the 1 ^{1}A" excited state the out–of–plane bending vibration of the molecule has a noticeable contribution to the lowering of the barrier to dissociation. Furthermore, our energy dissociation paths of the remaining 2 ^{1}A" and 1 ^{1}A' electronic excited states show that if the excitation process takes place without out–of–plane nuclear relaxation, the cleavage of HNO_3 to form OH· ($^2\Pi$) + NO_2· (1 $^2B_2$) can be described as an impulsed process. Further studies, to take into account the effects of the electronic distribution on the lowest photodissociation channels of the nitric acid are obviously needed and are under investigation in our group.

4 CONCLUSIONS

In this work, we use the density functional theory with its time–dependent (TD–DFT) formalism, in the study of the low–lying singlet and triplet excited states of nitric acid in gas–phase. Our results are in satisfactory agreement with UV experimental data and in analogy with previous results obtained by means of high level calculations and attest the proposed valence assignments of the main absorption bands; furthermore, the comparison with a more correlated and computationally demanding method, such as CASSCF and MCQDPT calculations further confirm the valuable performance of the TD–DFT formalism in the study of excited states dominated by one–electron transitions. Interestingly, in this work we show that at 248 nm, the potential energy barrier toward dissociation of the acid nitric in OH + NO_2 radical fragments strongly depends on the out–of–plane bending vibration of the molecule in the 1 ^{1}A" excited state having a noticeable contribution to the lowering of the barrier.

Acknowledgment

We gratefully acknowledge Prof. Massimiliano Aschi and Dr. Nico Sanna for stimulating discussions. Thanks are due to Dr. Andrea Pieretti and Dr. Andrea Grandi for computer facilities. This work has been supported to Supercomputing Center for University and Research (CASPUR).

5 REFERENCES

[1] C. Zazza, L. Bencivenni, M. Aschi, *Chem. Phys. Lett.* **2004**, *399*, 184.
[2] Y. Y. Bai, G. A. Segal, *J. Chem. Phys.* **1990**, *92*, 7479.
[3] A. M. Grana, T. J. Lee, M. Head–Gordon, *J. Phys. Chem.* **1995**, *99*, 3493.
[4] T. L. Myers, N. R. Forde, B. Hu, D. C. Kitchen, L. J. Butler, *J. Chem. Phys.* **1997**, *107*, 5361.
[5] G. H. Leu, C. W. Hwang, I. C. Chen, *Chem. Phys. Lett.* **1996**, *257*, 481.
[6] A. Sinha, R. L. Vander Wal, F. F. Crimm, *J. Chem. Phys.* **1989**, *91*, 2929.
[7] M. J. Krish, M. C. Reid, L. R. McCunn, R. J. Butler, J. Shu, *Chem. Phys. Lett.* **2004**, *397*, 21.
[8] A. McIlory, F. P. Tully, *J. Phys. Chem.* **1993**, *97*, 610.
[9] R. G. Parr, W. Yang, *Density Functional Theory of atoms and molecules*, Oxford Univ. Press **1989**.
[10] S. Hirata, M. Head–Gordon, *Chem. Phys. Lett.* **1999**, *302*, 375.
[11] R. E. Stratmann, G. E. Scuseria, M. J. Frisch, *J. Chem. Phys.* **1998**, *109*, 8218.
[12] C. Zazza, L. Bencivenni, A. Grandi, M. Aschi, *J. Mol. Struct.* (*THEOCHEM*), **2004**, *680*, 117.
[13] V. Barone, A. Palma, N. Sanna, *Chem. Phys. Lett.* **2003**, *381*, 451.
[14] C. Zazza, A. Amadei, N. Sanna, A. Grandi, G. Chillemi, A. Di Nola, M. D'Abramo, M. Aschi, *Phys. Chem. Chem. Phys.* **2006**, *12*, 1385.
[15] C. Zazza, A. Grandi, L. Bencivenni, M. Aschi, *J. Mol. Struct.* (*THEOCHEM*), **2006**, *764*, 87.
[16] A. D. Becke, *J. Chem. Phys.* **1986**, *84*, 4524.
[17] C. Lee, W. Yang, R. G. Parr, *Phys. Rev. B*, **1988**, *37*, 785.
[18] A. D. Becke, *J. Chem. Phys.* **1993**, *98*, 5648.
[19] J. P. Perdew, Y. Wang, *Phys. Rev. B* **1992**, *45*, 13244.
[20] J. P. Perdew, K. Burke, M. Ernzerhof, *Phys. Rev. Lett.* **1996**, *77*, 3865.
[21] M. Ernzerhof, G. E. Scuseria, *J. Chem. Phys.* **1999**, *110*, 5029.
[22] J. P. Perdew, K. Burke, Y. Wang, Phys. Rev. B **1996**, *54*, 16533.
[23] J. C. Slater, *Quantum Theory of Molecular and Solids. The Self–Consistent Field for Molecular and Solids*, vol. 4, McGraw–Hill, New York, **1974**.
[24] R. A. Kendall, T. H. Jr. Dunning, R. J. Harrison, *J. Chem. Phys.* **1992**, *96*, 6796.
[25] T. H. Jr. Dunning, *J. Chem. Phys.* **1989**, *90*, 1007.
[26] N. Nakano, *J. Chem. Phys.* **1993**, *99*, 7983.
[27] R. Krishnan, J. S. Binkley, R. Seager, J. A. Pople, *J. Chem. Phys.* **1980**, *72*, 650.
[28] M. J. Frisch, et al. Gaussian 03, Revision C.02, Gaussian, Inc., Wallingford, CT, **2004**.
[29] M. W. Schmidt, K. K. Baldridge, J. A. Boatz, S. T. Elbert, M. S. Gordon, J. H. Jensen, S. Koseki, N. Matsunaga, K. A. Nguyen, S. J. Su, T. L. Windus, M. Dupuis, J. A. Montgomery, *J. Comp. Chem.* **1993**, *14*, 1347.
[30] L. T. Molina, M. J. Molina, *Photochem.* **1981**, *15*, 97.
[31] O. Rattingan, E. Lutman, R. L. Jones, R. A. Cox, K. Clemitshaw, J. Williams, *J. Photochem. Photobiol. A: Chem.* **1992**, *66*, 313.
[32] C. Tuma, A. D. Boese, N. C. Handy, *Phys. Chem. Chem. Phys.* **1999**, *1*, 3939.
[33] J. Chase, W. Malcom, *NIST–JANAF Thermochemical Tables*, American Chemical Society, Washington, D.C., **1998**.